

REVIEW

Conformational Dynamics and Pre-Steady-State Kinetics of DNA Glycosylases

O. S. Fedorova*, N. A. Kuznetsov, V. V. Koval, and D. G. Knorre

*Institute of Chemical Biology and Fundamental Medicine, Siberian Branch of the Russian Academy of Sciences,
pr. Lavrent'eva 8, 630090 Novosibirsk, Russia; fax: +7 (383) 363-5153; E-mail: fedorova@niboch.nsc.ru*

Received March 10, 2010

Revision received April 30, 2010

Abstract—Results of investigations of *E. coli* DNA glycosylases using pre-steady-state kinetics are considered. Special attention is given to the connection of conformational changes in the interacting biomolecules with kinetic mechanisms of the enzymatic processes.

DOI: 10.1134/S0006297910100044

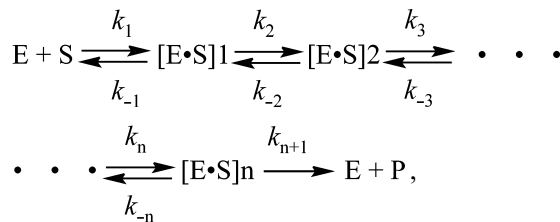
Key words: conformational dynamics, pre-steady-state kinetics, DNA glycosylases

Enzymatic processes involving proteins and DNA are often accompanied by conformational rearrangements of both these biopolymers [1-5]. However, the dynamics of the enzyme conformational changes and their connection with catalytic functions remain poorly studied [6-8]. Understanding the mechanisms of enzymatic reactions is mainly based on static structural data obtained from X-ray analysis and NMR spectroscopy, as well as on data of steady-state enzyme kinetics and structural analysis of intermediates and the substrate transformation products [9-11]. No doubt, these data contribute much to understanding the nature of enzymatic catalysis. However, these data are not enough to design a detailed molecular-kinetic model of an enzyme process.

Investigation of enzymatic reactions under steady-state conditions results in loss of a significant part of the information on the mechanism of the process and intermediate enzyme forms [12, 13]. Parameters of steady-state kinetics k_{cat} and K_{m} are complex functions of rate constants of all individual reactions occurring during an

enzymatic process [14]. Detailed kinetic investigations should include determination of all kinetic parameters of the interaction of the enzyme with the substrate. Direct determination of rate constants of elementary stages of a reaction can follow from analysis of pre-steady-state reaction kinetics.

A general case of reaction of substrate transformation to product with involvement of an arbitrary number n of intermediate complexes is shown in Scheme 1:



where E is enzyme, S is substrate, $[E \cdot S]_n$ are different enzyme-substrate complexes, P is reaction product, and k_i/k_{-i} here and further are rate constants that characterize stage i of the reaction. The kinetics of this process are described by the system of differential equations (1), the solution of which makes reveals the dependence of reaction member concentrations on time and initial concentrations of interacting substances. In the case when direct solution of the system of differential equations is impossible, then methods of numerical integration are used [15].

Abbreviations: AP, apurine/apyrimidine site; 2-aPu, 2-amino-purine; BER, base excision repair; F, 2-hydroxymethyl-3-hydroxy-tetrahydrofuran; Fpg, 8-oxoguanine-DNA glycosylase; MutY, adenine-DNA glycosylase; oxoG, 8-oxoguanine; ROS, reactive oxygen species; Trp, tryptophan; UDG, uracil-DNA glycosylase.

* To whom correspondence should be addressed.

$$\left. \begin{aligned}
 \frac{d[[ES]1]}{dt} &= k_1[S][E] + k_{-2}[[ES]2] - (k_{-1} + k_2)[[ES]1] \\
 \frac{d[[ES]i]}{dt} &= k_i[[ES](i-1)] + k_{-(i+1)}[[ES](i+1)] - (k_{-i} + k_{i+1})[[ES]i] \\
 &\vdots \\
 \frac{d[[ES]n]}{dt} &= k_n[[ES](n-1)] - (k_{-n} + k_{n+1})[[ES]n] \\
 \frac{d[P]}{dt} &= k_{n+1}[[ES]n] \\
 E_0 &= [E] + \sum_{i=1}^n [[ES]i] \\
 S_0 &= [S] + [P] + \sum_{i=1}^n [[ES]i]
 \end{aligned} \right\} (1)$$

If any reagent exists in excess over enzyme, the system can be integrated. Thus, if $S_0 \gg E_0$, then the substrate concentration can be considered as constant and bimolecular nonlinear member $k_1[E][S]$ can be replaced by $k_1[E]S_0$, which linearly includes just one variable concentration. In this case the system of $n + 1$ linear differential equations is obtained which is easily solved in a standard way by finding the roots of the n degree characteristic equation whose own values allow calculation of those of all rate constants [15]. Since the process takes place under conditions of multiple turnover of the enzyme, then after finishing pre-steady-state the period of time $t \gg \tau$ (τ is characteristic time of the slowest stage) the reaction is switched to steady state.

If it is possible to register all enzyme–substrate complexes and intermediates using any experimental technique, then it is reasonable to carry out this reaction in a single enzyme turnover ($E_0 \geq S_0$) and pre-steady-state conditions. In this case the system of differential equations has to be solved numerically (1). However, all stages of the enzymatic process can be characterized in this case [14, 15].

Thus, investigation of pre-steady-state kinetics allows detailed analysis of the mechanism of an enzymatic reaction. Although this approach is technically more complicated and its usage requires more laborious mathematical analysis, investigation of enzymatic reactions in pre-steady-state conditions provides deeper knowledge concerning the mechanisms of enzyme action [16, 17].

Such methods of pre-steady-state kinetics as “quench-flow” and “stopped-flow” are used in investigation of enzymatic processes. Both methods are based on rapid (~ 1 msec) mixing the interacting substances and discontinuation of reaction mixture flow. The interruption of the reaction in the “quench-flow” method takes place either upon rapid freezing of the reaction mixture or upon mixing with quenching agents. Analysis of reaction mixture composition at different moments from the reaction start within time interval of the order 1–1000 msec makes it possible to obtain kinetic dependences for intermediates and end products. In the “stopped-flow”

method changes in substance concentrations during chemical reaction are usually registered by optical methods such as optical absorption or fluorescence.

Tryptophan (Trp) is the most intensely fluorescent amino acid [18] and $\sim 90\%$ of total protein fluorescence is usually due to Trp. The maxima of protein fluorescence emission depend on the local environment of Trp residues in a polypeptide molecule. For example, a shift to shorter wavelength is interpreted as the result of shielding of Trp residues against the aqueous phase. Thus, the denaturation of a protein results in a shift in the fluorescence emission spectrum to longer wavelengths resulting in approximately the same maximum in the emission spectra of all proteins. The properties of Trp can be used as a highly sensitive fluorescent marker of conformational changes in protein molecules [19–21]. However, it is necessary to keep in mind that most proteins contain several Trp residues located in different environments, and therefore the spectral properties of each of them can be different.

Fluorescent properties of macromolecules often do not reveal desired information from an experiment. In some cases it is possible to overcome this difficulty using fluorophores, even though they are foreign relative the system under study, but have better spectral properties. For example, in investigation of enzymatic reactions with involvement of nucleic acids, fluorescent nucleotide analogs are used, which in this case retain the ability to hydrogen bond with unmodified nucleotides. Conformational transitions in DNA molecule are usually registered by changes in fluorescence intensity of 2-aminopurine (2-aPu). The 2-aPu residue is one of most attractive fluorescent analogs of heterocyclic bases. As in the case with adenine, two hydrogen bonds are formed in the 2-aPu/T pair, and both one and two hydrogen bonds can be simultaneously formed in the 2-aPu/C pair [22, 23]. Thus incorporation of a 2-aPu residue opposite C and T bases results in minimal distortions of the DNA structure. Fluorescence intensity of 2-aPu is very strongly dependent on the environment. Thus, the existence of stacking interactions between adjacent bases or upon formation of double-helical DNA structures sharply decreases the fluorescence intensity of 2-aPu residues [24]. The sensitivity of 2-aPu fluorescence to conformational changes in the DNA double helix is the basis for the use of this base analog in investigation of enzyme interactions with DNA. 2-Aminopurine was used to study kinetic characteristics of different enzymes interacting with DNA, such as DNA polymerase I Klenow fragment [25], DNA polymerases β and λ [19, 26], bacteriophages T7 RNA polymerase [27], DNA polymerases of bacteriophages T4 and RB69 [28, 29], DNA methyltransferases [30], DNA glycosylases [21], and other enzymes.

Results of kinetic studies of DNA glycosylases involved in DNA repair are considered in this review. Special attention is given to the relationship between interacting molecules and their conformational changes

with the reaction kinetic mechanism and to elucidation of the role of separate elementary stages in the course of an enzymatic process.

DNA of living organisms is constantly influenced by various factors including highly reactive cell metabolites, UV- and ionizing radiation, etc. Oxidation, alkylation, deamination, apurination/apyrimidination, and formation of breaks in DNA are only some of the processes leading to damage to DNA structure [31–34]. Similar damages of the genetic apparatus exhibit cytotoxic and mutagenic effects and cause different diseases [35–39]. Oxidative lesions of cellular macromolecules also accelerate development of degenerative processes in the organism [40, 41].

All living organisms are able to repair damages and restore initial DNA structure [42–44]. It is assumed that on the pathway of base excision repair (BER) most damages in DNA heterocyclic bases and AP sites are eliminated [45–47].

The overall BER mechanism includes elimination of a damaged heterocyclic base, deoxyribose residue, and phosphate, as well as subsequent restoration of the excised nucleotide by the cell replicative machine [48, 49]. The damaged or incorrectly paired bases are removed by DNA glycosylases. Most of these are able to remove several different modified bases. They include two types of enzymes—mono- and bifunctional. Bifunctional DNA glycosylases catalyze two successive reactions, glycoside bond cleavage with formation of a free base and subsequent breakage of the phosphodiester bond from the side of the 3' carbon atom of a 2'-deoxyribose residue by β -elimination (AP-lyase activity) by forming a nick in DNA. Besides, some bifunctional DNA glycosylases are able to carry out the second reaction of β -elimination resulting in breakage of the phosphodiester bond at the 5' carbon atom and removal of a 2'-deoxyribose residue. Unlike them, monofunctional DNA glycosylases cleave only an *N*-glycoside bond with formation of a modified base and AP site [50, 51]. Then apurine/apyrimidine endonucleases remove the remaining deoxyribophosphate residue [47, 52]. The formed gap of a single nucleotide contains at the 3' end hydroxyl group and phosphate residue at the 5' end. DNA polymerase joins the necessary nucleotide and DNA ligase terminates the BER process by restoration of integrity of the deoxyribophosphate backbone.

DNA glycosylases that recognize different modified and incorrectly paired bases and catalyze cleavage of the *N*-glycoside bond with damaged nitrogen base certainly play the main role in base excision repair [53, 54]. Their purpose is to detect quickly and precisely the modified base among numerous undamaged nitrogen bases and to initiate the repair process [55].

Comparison of numerous structures of DNA glycosylases distinguishes four families, three of which are UDG, AAG, and MutM/Fpg in accordance with structural similarity to uracil-DNA glycosylase, alkyladenine-

DNA glycosylase, and bacterial 8-oxoguanine-DNA glycosylase, respectively [56–58]. The fourth family is called HhH-GPD because active centers of enzymes of this family contain a sequence that forms a helix–hairpin–helix (HhH) structure, followed by a loop containing glycine, proline, and aspartate residues (GPD) [59]. Although DNA glycosylases of different families are structurally different, they exhibit common features upon interaction with substrates. Thus, all DNA glycosylases with presently established structure evert the damaged base and transfer it into the enzyme active center [55].

Investigation of DNA glycosylase chemical stages leads to a common model of the catalytic mechanism. Monofunctional DNA glycosylases catalyze hydrolysis of a glycoside bond by the S_N1 mechanism with formation of an apurine/apyrimidine site. Unlike them, bifunctional DNA glycosylases catalyze attack of the 1' carbon atom by the amino group of the enzyme lysine residue by the S_N2 mechanism [60]. The attack by the nucleophilic amino group results in Schiff base formation between the 1' carbon atom of 2'-deoxyribose and the enzyme. Redistribution of electron density results in cleavage of the bond between the 3' carbon atom of the 2'-deoxyribose and phosphate group via the β -elimination mechanism. Then the Schiff base is hydrolyzed with the release of the free enzyme form and the polynucleotide strand is broken with formation of α,β -unsaturated aldehyde at the 3' end and phosphate at the 5' end and with formation of a break in the DNA molecule containing α,β -unsaturated aldehyde at the 3' end and phosphate at the 5' end. After finishing the first reaction of β -elimination, some enzymes, such as formamidopyrimidine-DNA glycosylase Fpg, carry out the second β -elimination reaction [60]. This results in a single nucleotide break in the DNA sequence with phosphates at its 3' and 5' ends [60].

In recent years many data on DNA glycosylase structures and complexes with intermediates and substrates have been obtained (reviews [56–58]). However, despite success in structural and biochemical investigations of some DNA glycosylases, the available data are not enough for producing a detailed concept concerning mechanisms of searching by enzymes for damaged bases and their following elimination from DNA. Considerable contribution to understanding of these mechanisms can be made by studies of pre-steady-state kinetics of the process with recording of conformational transitions in enzymes and DNA substrates. Such investigations have been carried out for *E. coli* bifunctional DNA glycosylases (uracil-, adenine-, and formamidopyrimidine-DNA glycosylases) that will be considered in following section.

E. coli URACIL-DNA GLYCOSYLASE

The main source of uracil in DNA is deamination of cytosine resulting in formation of a G-U pair. Replication

of DNA containing such base pair results in the G-C \rightarrow A-T mutation. Uracil is repaired in DNA by the pathway of uracil excision by uracil-DNA glycosylase [61].

Structures of *E. coli*, human, and type 1 herpes simplex virus uracil-DNA glycosylases have been determined [62-65]. It has been shown that in the enzyme-DNA catalytic complex uracil is extruded from the duplex and is localized in the active center of the glycosylase. A leucine

residue (Leu272 and Leu191 in human and *E. coli* enzymes, respectively) is localized in the formed cavity of the DNA double helix. Structural data obtained in [62-64] revealed stages of the mechanism of interaction of uracil-DNA glycosylase with DNA. In the first stage the noncovalent binding of the enzyme to DNA results in local structural distortions in interacting molecules. Such distortions result in the uracil base eversion from the

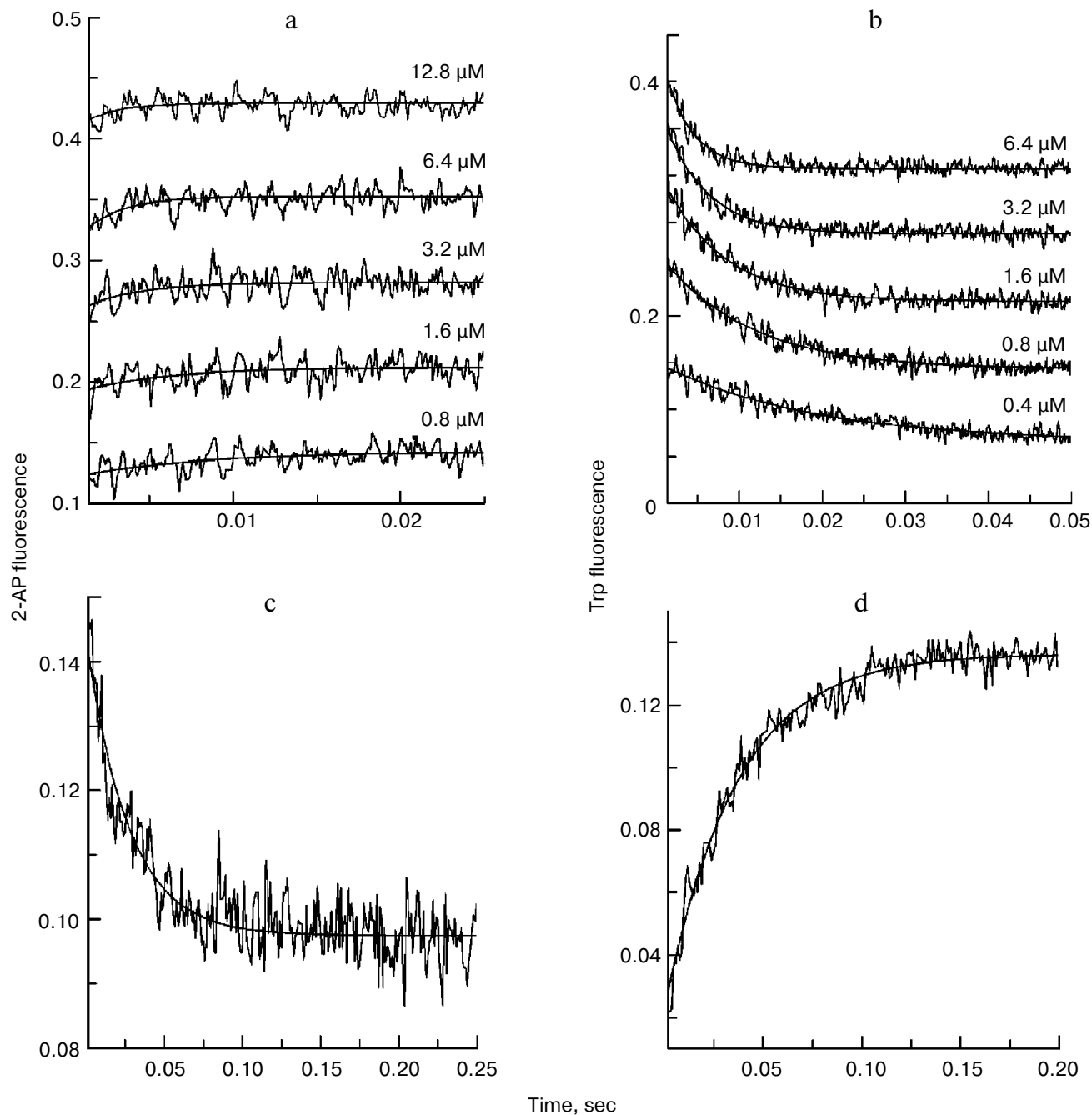
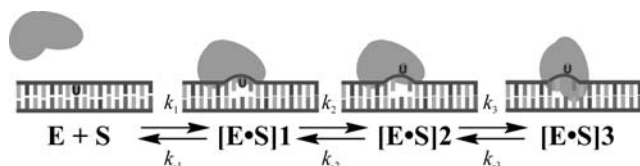


Fig. 1. Kinetic curves that characterize stages of binding of UDG to DNA (a, b) and stages of enzyme-DNA complex dissociation (c, d) upon recording 2-aPu (a, c) or Trp (b, d) fluorescence [68]. Reprinted with permission from paper of Y. L. Jiang and J. T. Stivers (*Biochemistry* (2002) **41**, 11236-11247). Copyright 2002 American Chemical Society.

DNA duplex and following occupation of its place by a leucine residue. Then the *N*-glycoside bond between uracil and the ribose residue is cleaved. The enzymatic process is completed by the dissociation of the enzyme–product complex.

The kinetic mechanism of the enzymatic reaction of *E. coli* UDG has been studied by many authors [21, 66–68]. The stage of UDG binding to DNA substrate was studied in detail by Jiang and Stivers [68]. Substrates containing 2'- β -fluoro-2'-deoxyribouridine were used to block the catalytic stage of the process. Conformational changes in the protein were monitored by changes in Trp fluorescence intensity. Stages of DNA helix distortion and uracil extrusion were registered by changes in fluorescence of 2-aPu localized opposite uracil. Kinetic curves in Fig. 1 show that complex formation between UDG and DNA results in an increase in the 2-aPu fluorescence intensity and decrease in that of Trp. The stages of enzyme–DNA complex dissociation are characterized by decrease in 2-aPu fluorescence intensity and increase in Trp fluorescence.

Kinetic curves obtained in [68] revealed three conformational transitions in the *E. coli* UDG molecule. Data obtained by these and other authors on enzyme structures and complexes with substrate [64, 65] suggested a kinetic mechanism of substrate binding by UDG. Enzyme–substrate complexes formed during the reaction are shown in Scheme 2:



where E is enzyme, S is substrate, $[E \cdot S]n$ are different enzyme–substrate complexes, k_i and k_{-i} are rate constants characterizing the *i*th reaction step. Reaction rate constants corresponding to Scheme 2 are given in Table 1. It was found that after enzyme binding to DNA (step 1), characterized by rate constants k_1 , close to the diffusion limit, and k_{-1} , local distortion of DNA structure occur that result in rapid eversion of uracil from the duplex (step 2). Then conformational changes in enzyme structure occur, which result in formation of the catalytically active state (step 3).

The role of all amino acid residues involved in the interaction of UDG with the damaged DNA site was also determined [68]. It was shown that residues Ser88 and Ser189 interacting with phosphate groups at the 5' and 3' uridine ends take part in initial deformation of the DNA duplex resulting in shortening the P–P distance or to strand “pinching” (the $[E \cdot S]1$ complex in Scheme 2). Besides, they are necessary at a later step of stabilization of the catalytically active state. Residues Asn123 and His187 form the network with uracil and are responsible

Table 1. Rate constants corresponding to Scheme 2 [68]

Constant	Value
$k_1, \mu\text{M}^{-1}\cdot\text{sec}^{-1}$	220 ± 50
k_{-1}, sec^{-1}	600 ± 100
k_2, sec^{-1}	700 ± 200
k_{-2}, sec^{-1}	180 ± 50
k_3, sec^{-1}	350 ± 50
k_{-3}, sec^{-1}	100 ± 10

for the base eversion from the DNA duplex (complex $[E \cdot S]2$ in Scheme 2). Substitution of glycine for these amino acids (especially for Asn123) retarded the stage of uracil eversion. The role of Leu191, occupying the place of the extruded uracil in the DNA duplex, underwent the most thorough analysis because there are several possible variants of action of this amino acid. On one side, Leu191 can “push” uracil from double helix; on the other side, it can penetrate the duplex after uracil extrusion and thus stabilize the extra-helical position of the base (“plug”). Replacement of leucine by alanine or glycine resulted in sharp decrease of rate constant of the $[E \cdot S]2$ complex formation (see Scheme 2), which is indicative of the “push” effect of this residue.

Results reported in [68] significantly contributed to overall understanding of the elementary stages of the process of DNA binding by *E. coli* UDG. However, the most detailed kinetic mechanism known as “pinch–pull–push” and including steps of the enzymatic process such as substrate binding, catalysis, and dissociation of reaction product was proposed in [21]. A 27-membered DNA duplex containing uracil in one of its chains and 2-aminopurine or adenine opposite it in the complementary chain was used for investigation in this work. Parallel recording of the Trp and 2-aPu fluorescence intensities revealed the sequence of elementary steps during the reaction. Kinetic curves in Fig. 2 show that the increase in 2-aPu fluorescence intensity upon the interaction of UDG with the substrate takes place during the first 10 msec, which is characteristic of uracil extrusion from DNA. Within time interval from 5 to 20 msec the Trp fluorescence intensity increased. Since the authors of [21] associated conformational changes in the protein with translocation of the Leu191 residue, such character of the curves suggested that the penetration of the Leu191 residue into the DNA strand occurred after the extrusion of uracil.

Data obtained by Wong et al. [21] allowed the authors to suggest the kinetic mechanism of action for *E. coli* uracil–DNA glycosylase and to determine rate constants

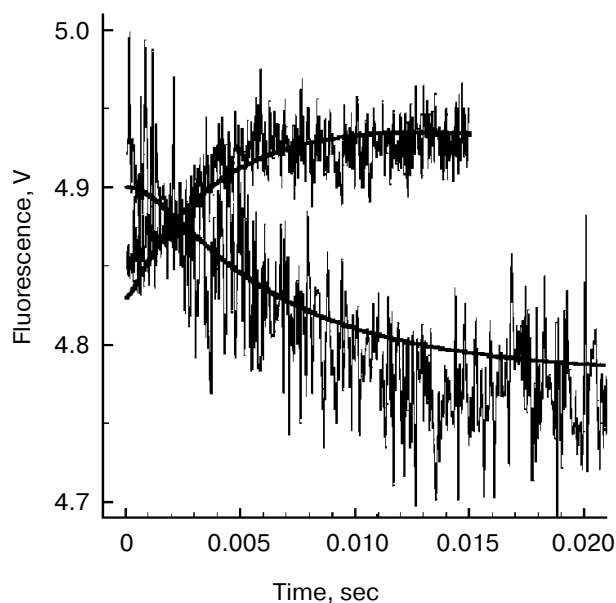


Fig. 2. Kinetic curves characterizing uracil eversion (increase of fluorescence intensity) and insertion of Leu191 from *E. coli* UDG into the DNA duplex (decrease of fluorescence intensity) [21]. Reprinted with permission from paper of I. Wong, A. J. Lundquist, A. S. Bernards, and D. W. Mosbaugh (*J. Biol. Chem.* (2002) 277, 19424–19432). Copyright 2002 American Society for Biochemistry and Molecular Biology.

corresponding to this mechanism (Scheme 3 and Table 2). The sequence of processes during the interaction of the enzyme with the substrate is as follows. DNA substrate binding to enzyme with formation of $[E \cdot S]1$ complex included the chain “pinch” followed by uracil “pull” from the duplex (complex $[E \cdot S]2$). Then the Leu191 residue was inserted into the formed DNA cavity (“push”). This was followed by conformational transition in the enzyme molecule and formation of catalytically active complex $[E \cdot S]3$ in which the chemical stage of the process, the breakage of the *N*-glycoside bond, took place and the $[E \cdot P]$ complex was formed. The leucine residue reverse pulling out from the DNA, formation of $[E \cdot P]1$ complex, and its dissociation completed the enzymatic cycle.

In conclusion, the kinetic and structural data together with results of site-directed mutagenesis revealed the

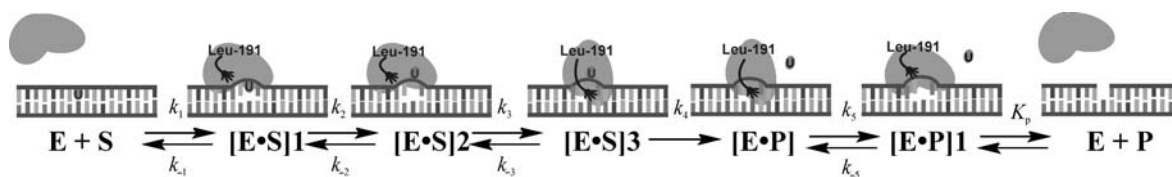
detailed mechanism of the interaction of *E. coli* uracil-DNA glycosylase UDG with DNA. The reaction scheme described in [21] characterizes all changes in enzyme and substrate conformation that occur after removal of uracil from DNA and represent the first complete model describing the whole enzymatic cycle of this DNA glycosylase.

E. coli ADENINE-DNA GLYCOSYLASE MutY

Products of the action of reactive oxygen species (ROS) (e.g. O_2^- , H_2O_2 , and $\cdot OH$) are among the most common DNA damages. ROS are generated in living organisms during cell respiration. They can also emerge in response to ultraviolet or ionizing radiation and to various chemical agents. The action of ROS on DNA results in modification of nitrogen bases, formation of single or double strand DNA breaks, apurine/apyrimidine sites, and covalent bonds with proteins [69, 70]. The main products of purine base modifications are 7,8-dihydro-8-oxoguanine (8-oxoguanine, oxoG) and formamidopyrimidine derivatives of adenine (4,6-diamino-5-formamidopyrimidine, Fapy A) and guanine (2,6-diamino-4-oxy-5-formamidopyrimidine, Fapy G) [71, 72].

The oxoG base can form during replication of a Hoogsteen pair with adenine (oxoG/A pair). The following replication results in mutation G/C \rightarrow T/A [73, 74]. To counteract oxoG accumulation, living organisms have a special protective system (GO system) [75, 76] counteracting oxoG accumulation. This system is well characterized in *E. coli*. It consists of three enzymes: Fpg (MutM), a specific *N*-glycosylase/AP-lyase removing oxoG residues; MutY, a specific *N*-glycosylase removing an adenine residue opposite oxoG, and MutT, a specific phosphatase active against 8-oxo-dGTP. Most eukaryotic organisms have structural or functional homologs of these bacterial enzymes [77, 78].

Adenine-DNA glycosylase plays the key role in repair of DNA containing the A/oxoG pair [79, 80]. Crystal structures of MutY from *E. coli* and *B. stearothermophilus* in the free state and in complex with DNA are now available [81–83]. Features of DNA substrate binding were revealed by X-ray analysis, and it was shown that in



Kinetic mechanism of action for *E. coli* uracil-DNA glycosylase. Designations: E is UDG enzyme from *E. coli*, S is DNA substrate, $[E \cdot S]1$ is enzyme–DNA substrate complex, $[E \cdot S]2$ is enzyme complex with DNA substrate in which uracil is extruded from the duplex, $[E \cdot S]3$ is catalytically active enzyme–DNA substrate complex, $[E \cdot P]$ and $[E \cdot P]1$ are enzyme complexes with reaction product

Scheme 3

Table 2. Rate and equilibrium constants corresponding to Scheme 3

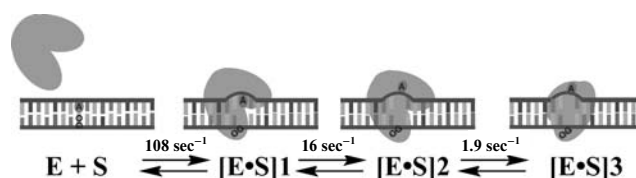
Number	Reaction	k_n	k_{-n}
1	Nonspecific binding ("pinch")	$\geq 1.8 \cdot 10^{10} \text{ M}^{-1} \cdot \text{sec}^{-1}$	5000 sec^{-1}
2	Uracil "pull"	$1100 \pm 70 \text{ sec}^{-1}$	$350 \pm 30 \text{ sec}^{-1}$
3	Incorporation of Leu191 residue ("push")	$300 \pm 30 \text{ sec}^{-1}$	$170 \pm 50 \text{ sec}^{-1}$
4	Cleavage of <i>N</i> -glycoside bond	$58 \pm 4 \text{ sec}^{-1}$	0
5	Reverse pulling out of Leu191 residue	$35 \pm 4 \text{ sec}^{-1}$	$25 \pm 5 \text{ sec}^{-1}$
	Steady-state k_{cat} (product dissociation)	$0.5 \pm 0.08 \text{ sec}^{-1}$	

catalytically active complex adenine is extruded from the DNA duplex to the enzyme active center, whereas a number of specific contacts are established with the oxoG base.

Crystallographic studies of enzyme and its complexes with DNA also clarified the mechanism of MutY action that for a long time could not be unambiguously classified as mono- or bifunctional DNA glycosylase [84–86]. Now an enzymatic reaction mechanism has been proposed in which the *N*-glycoside bond is broken upon attack by a water molecule (monofunctional type of DNA glycosylases) [87, 88]. The formed AP site generates a Schiff base with the amino group of Lys142, which makes possible the reaction of β -elimination (Fig. 3).

The pre-steady-state characteristics of *E. coli* MutY binding to DNA duplex containing the A/oxoG pair was investigated by Bernards et al. [71]. The stop-flow technique with recording of 2-aminopurine fluorescence intensity was used. The authors studied three 21-membered duplexes whose central part carried sequences (2-aPu)AT:A(oxoG)T, AAT:(2-aPu)(oxoG)T, and ACT:(2-aPu)(oxoG)T. Their kinetic curves are shown in Fig. 4. It is seen that in the case of AAT:(2-aPu)(oxoG)T substrate, 2-aPu fluorescence intensity rapidly increases during 50 msec. They explained this by disappearance of stacking between 2-aPu and oxoG bases and suggested that at this moment the oxoG residue is extruded from the DNA strand into the enzyme active center with rate constant 108 sec^{-1} . The change in the 2-aPu residue fluorescence intensity in the case of (2-aPu)AT:A(oxoG)T substrate (Fig. 4) indicates the extrusion of adenine from the helix and is characterized by the rate constant 16 sec^{-1} . They also distinguished in this kinetic curve an additional phase of the fluorescence intensity change with rate constant 1.9 sec^{-1} . By analogy with uracil-DNA glycosylase, this process was explained by a change in enzyme conformation resulting in stabilization of the extruded state of adenine. The ACT:(2-aPu)(oxoG)T duplex was used as a control of the MutY enzyme specificity because the oxoG:C pair is not a substrate for this enzyme.

Scheme 4 shows the sequence of stages occurring during DNA substrate binding by the enzyme (proposed in [71]):



where E is MutY enzyme from *E. coli*, S is DNA substrate carrying pair A:oxoG, [E • S]1 is the enzyme complex with DNA substrate in which recognition of A:oxoG pair and duplex distortion take place, [E • S]2 is the enzyme complex with DNA substrate in which adenine base is extruded from the duplex, [E • S]3 is catalytically active enzyme complex with DNA substrate in which enzyme isomerization is occurring. With account of data from [82], the first stage should be attributed to the process of DNA duplex distortion rather than oxoG extrusion. Formation of catalytically active complex results in the catalytic stage of the reaction with rate constant 0.25 sec^{-1} .

Data obtained [82] in the crystallographic study of the enzyme–substrate complex showed that during catalytically active complex formation no oxoG residue extrusion from the DNA helix takes place. Evidently, at the first stage just the DNA bending rather than oxoG extrusion occurs.

In kinetic studies of other authors [89–91] much attention was paid to determination of rate constants of catalytic stage and dissociation of the enzyme–product complex. The rate constant of the *N*-glycosylase reaction was 10 min^{-1} ($\sim 0.17 \text{ sec}^{-1}$), close to $0.25 \pm 0.03 \text{ sec}^{-1}$ reported in [71]. Besides, it was found that dissociation of the enzyme–product complex is the rate-limiting stage of the whole enzymatic process. In all three works [80–82] this stage is characterized by a rate constant in the range of $0.004\text{--}0.007 \text{ min}^{-1}$.

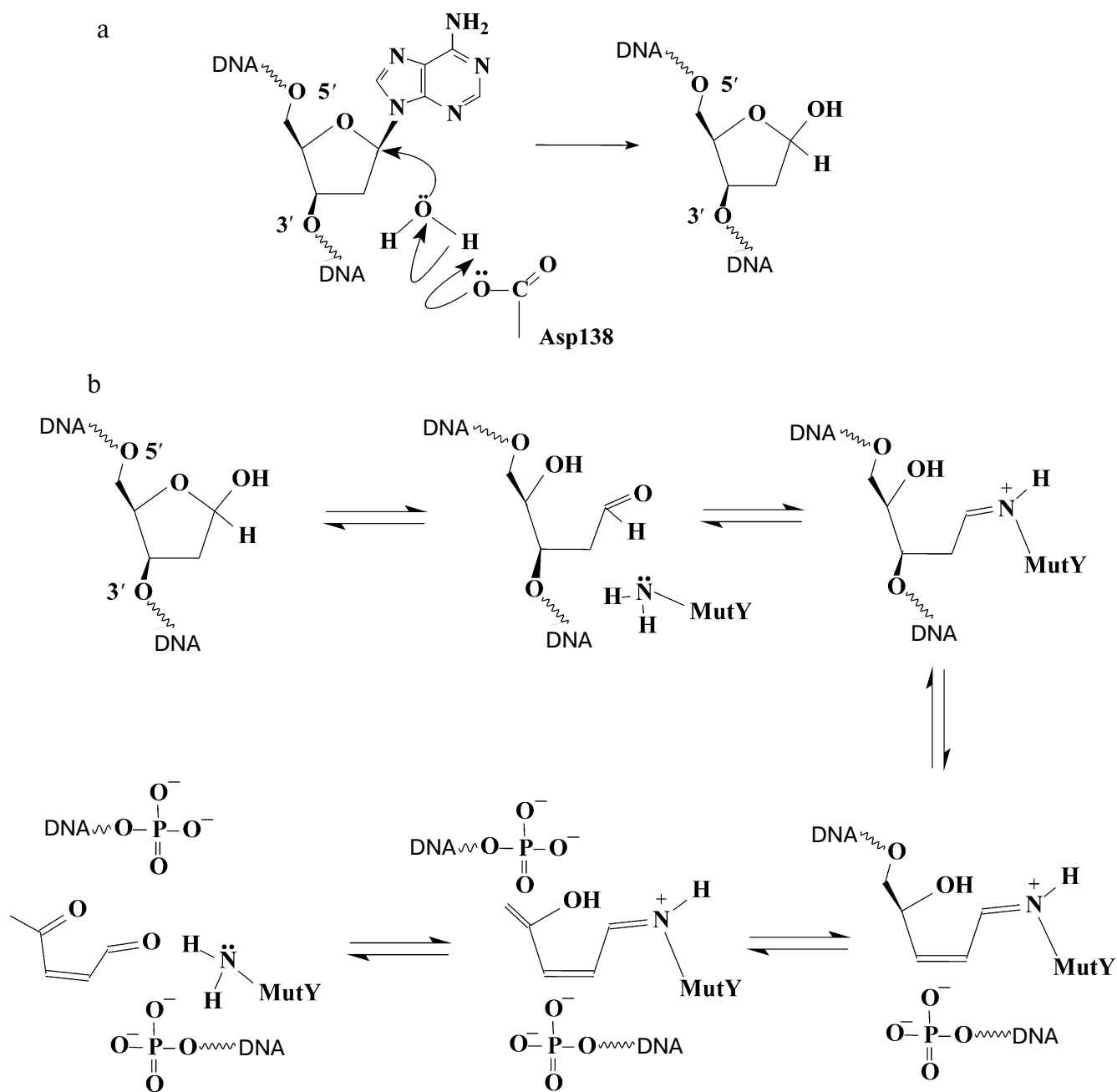


Fig. 3. Schematic presentation of catalytic reactions responsible for *N*-glycosylase (a) and AP-lyase (b) activities of *E. coli* MutY [88]. Modified with permission from paper of R. C. Manuel, K. Hitomi, A. S. Arvai, P. G. House, A. J. Kurtz, M. L. Dodson, A. K. McCullough, J. A. Tainer, and R. S. Lloyd (*J. Biol. Chem.* (2004) **279**, 46930-46939). Copyright 2004 American Society for Biochemistry and Molecular Biology.

Thus, the detailed kinetic mechanism was proposed on the basis of kinetic and structural investigations for the interaction of *E. coli* adenine-DNA glycosylase MutY with DNA substrates containing the A/oxoG pair. Results of works [71, 82] show that conformational changes occurring in both interacting molecules during substrate recognition and binding result in formation of a catalytically active complex and the enzymatic reaction.

E. coli 8-OXOGUANINE-DNA GLYCOSYLASE Fpg

Protein Fpg (MutM) is one of the enzymes of the *E. coli* bacterial GO system. This protein is a bifunctional enzyme that cleaves the *N*-glycoside bond of a damaged base with formation of an AP site and free oxoG. Then it breaks the phosphodiester bond from the side of the 3' carbon atom of the 2'-deoxyribose residue by β -elimina-

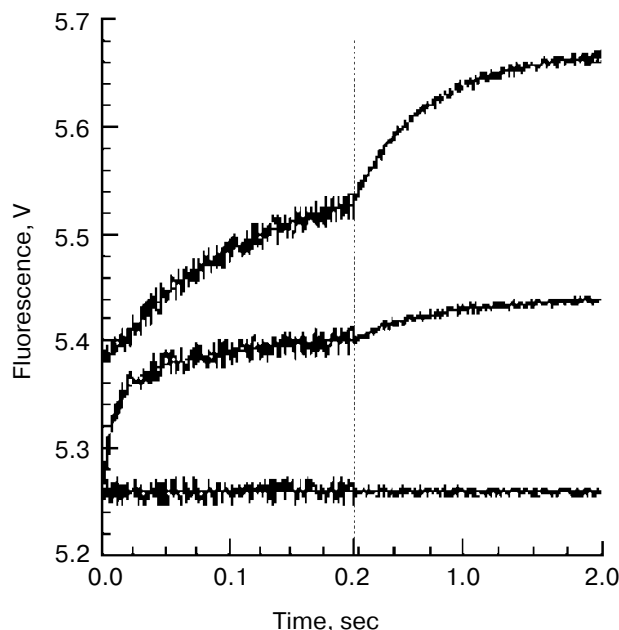


Fig. 4. Kinetic curves obtained on the interaction of *E. coli* adenine-DNA glycosylase MutY with DNA substrates ([MutY] = 500 nM, [DNA substrate] = 250 nM) [71]. Reprinted with permission from paper of A. S. Bernards, J. K. Miller, K. K. Bao, and I. Wong (*J. Biol. Chem.* (2002) **277**, 20960-20964). Copyright 2002 American Society for Biochemistry and Molecular Biology.

tion via Schiff base formation with the terminal Pro1 residue (AP lyase reaction), thus forming the single-stranded break in the DNA. Then the Fpg enzyme catalyzes the second β -elimination reaction, which results in removal of the ribose residue in the form of 4-oxo-2-pentenal and formation of a single-nucleotide gap with the phosphate group residues at the 3' and 5' DNA ends [92-94] (Fig. 5).

X-Ray studies [95] showed that the interaction of Fpg with DNA substrates results in conformational changes in protein. In this case the damaged oxoG base extrudes from the DNA helix into the enzyme active center with translocation into the vacated region of amino acid residues Met73, Arg108, and Phe110. Besides, bending of the DNA ribose-phosphate backbone is observed. Such structural changes in interacting molecules lead to formation of specific contacts resulting in highly efficient recognition and binding of damaged DNA regions. Figure 6 presents the overall structure of Fpg adduct with the DNA AP site in the form of a Schiff base formed by the Pro1 residue and the C1' atom of ribose after reduction by sodium borohydride [95].

In the series of works [96-98] conformational changes in enzymes and DNA were followed by changes in fluorescence intensity of tryptophan (Trp) and 2-aminopurine (2-aPu) residues, respectively, in real time

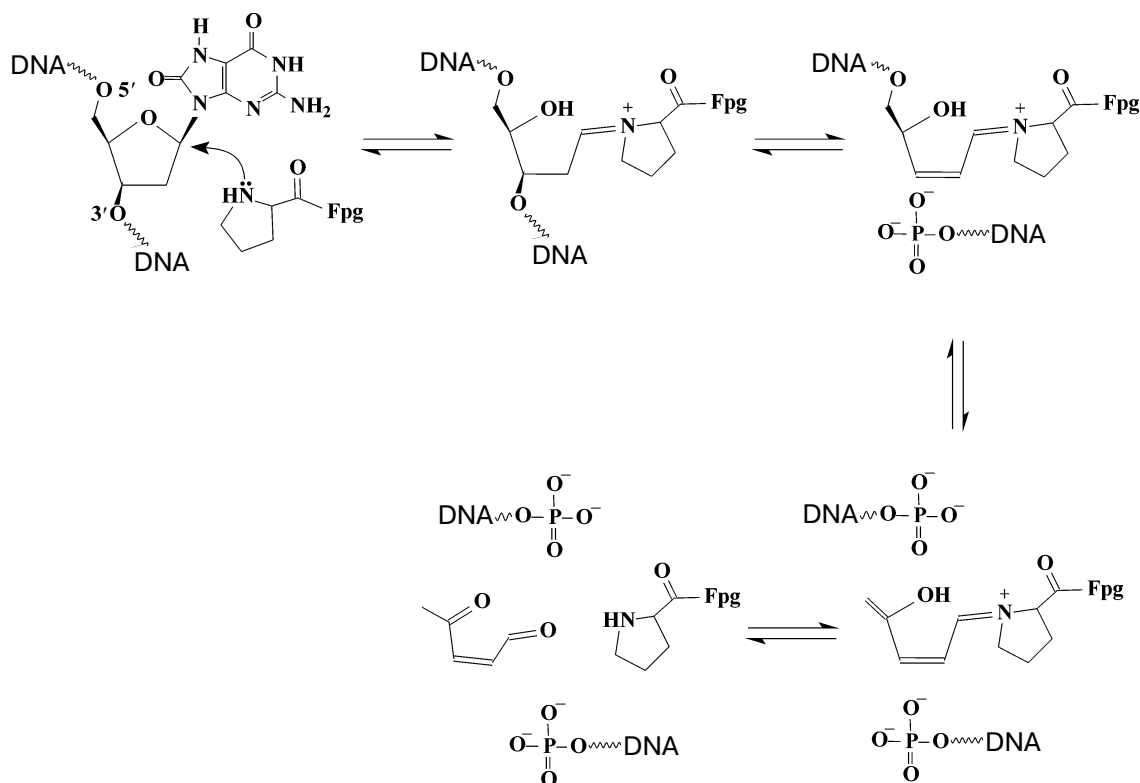


Fig. 5. Chemical mechanism of action of *E. coli* Fpg [93]. Reprinted with permission from paper of D. O. Zharkov, R. A. Rieger, C. R. Iden, and A. P. Grollman (*J. Biol. Chem.* (1997) **272**, 5335-5341). Copyright 1997 American Society for Biochemistry and Molecular Biology.



Fig. 6. Structure of Fpg enzyme complex with DNA substrate (PDB ID 1K82).

using the stopped-flow technique under conditions of single enzyme turnover.

To elucidate the nature of the enzymatic stages accompanied by conformational changes in the enzyme and DNA, 12-membered duplexes containing residues or AP site, formed as an intermediate during the first catalytic stage, and its non-reactive analog, a tetrahydrofuran F residue. Duplex with undamaged G residue was used as the control (Table 3).

Such stage-by-stage substrate complication consisting in transition from nonspecific DNA duplex (G ligand, the simplest interactions) to specific oxoG substrate (complete enzymatic cycle) made possible to follow conformational changes occurring in the enzyme and substrate molecules. X-Ray data that appeared in the literature during investigation [95] gave the possibility to identify the detailed molecular-kinetic mechanism

of the interaction of *E. coli* Fpg with DNA substrates [96-98].

Figure 7 shows kinetic curves that describe changes in Trp fluorescence intensity in Fpg and thus characterizing conformational changes in Fpg upon its interactions with DNA substrates, and respectively, in changes of 2-aPu fluorescence intensity characterizing conformational changes in DNA. The interaction of Fpg with nonspecific ligand, oligonucleotide duplex free of modified nucleotides (G ligand) resulted in nonspecific complex formation. This process is described by equilibrium: $E + G \leftrightarrow E \cdot G$.

It is seen in Fig. 7a (curve G^{Trp}) in the case of non-specific complex formation during 3 msec, that the enzyme structure is changed. These changes also result in "loosening" of the DNA duplex, which is characterized by increase in 2-aPu fluorescence intensity during 5 msec (Fig. 7a, curve $G\text{-aPu}^{2\text{-aPu}}$).

Kinetic curves of changes in Trp fluorescence intensity upon the interaction of Fpg with F ligand have more complex profile and characterize the process of primary binding and further rearrangement of the enzyme conformation (Fig. 7b, curve F^{Trp}). Four time regions can be distinguished in the changes in Trp fluorescence intensity. The first (2-20 msec) is characterized by decrease in fluorescence intensity, the second (40-100 msec) by its growth, the third (0.1-3.0 sec) and fourth (5-70 sec) by repeated fall. The kinetic scheme satisfying these data includes four equilibrium stages (Scheme 5):



For non-reactive fluorescent analog of AP substrate, ligand F, there appeared decrease in 2-aPu fluorescence intensity (Fig. 7b, curve $F\text{-aPu}^{2\text{-aPu}}$) at times below 2.0 sec, which is described by the single-stage equilibrium $E + F \leftrightarrow E \cdot F$ and can be due to penetration of the enzyme amino acid residues into the duplex.

Table 3. Oligonucleotide sequences of DNA substrates

Abbreviation	Oligonucleotide sequence
oxoG	d(CTCTC(oxoG)CCTTCC)/d(GGAAGGCGAGAG)
oxoG-aPu	d(CTCTC(oxoG)(2-aPu)CTTCC)/d(GGAAGCCGAGAG)
aPu-oxoG	d(CTCT(2-aPu)(oxoG)CCTTCC)/d(GGAAGGCCAGAG)
AP	d(CTCTC(AP)CCTTCC)/d(GGAAGGCGAGAG)
AP-aPu	d(CTCTC(AP)(2-aPu)CTTCC)/d(GGAAGCCGAGAG)
F	d(CTCTCFCTTCC)/d(GGAAGGCGAGAG)
F-aPu	d(CTCTCF(2-aPu)CTTCC)/d(GGAAGCCGAGAG)
G	d(CTCTCGCCTTCC)/d(GGAAGGCGAGAG)
G-aPu	d(CTCTCG(2-aPu)CTTCC)/d(GGAAGCCGAGAG)

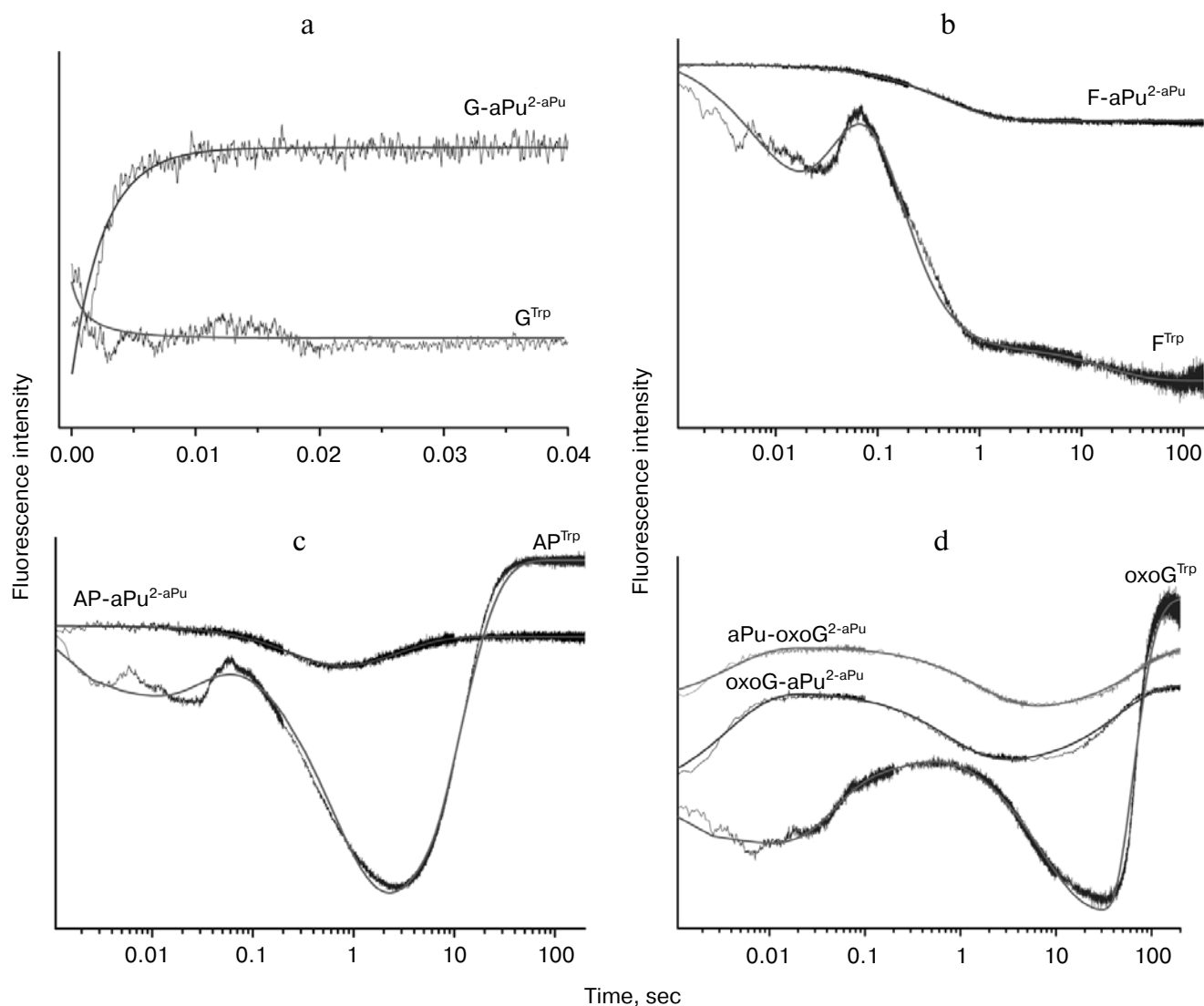


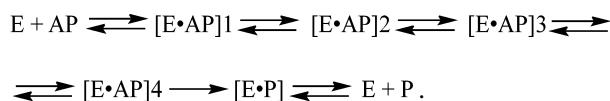
Fig. 7. Experimental kinetic curves that characterize conformational changes in Fpg (index Trp) and DNA substrates (index 2-aPu) upon their interaction and curves calculated using proposed schemes. a) G ligand; b) F ligand; c) AP substrate; d) oxoG substrate.

According to X-ray data [95] these are residues Met73, Arg108, and Phe110 (Fig. 6). It is seen in Fig. 7b that the two-phase change in Trp fluorescence intensity corresponds to the single-phase change in the 2-aPu fluorescence intensity in the region 0.03–0.3 sec. This means that incorporation of the three amino acid residues is probably not simultaneous and results in two-phase change in Trp fluorescence intensity. Evidently, just in the [E • F]3 complex complete incorporation of amino acids into DNA double helix occurs. The last, fourth stage resulting in formation of [E • F]4 complex and insignificantly influencing Trp fluorescence is apparently a re-adjustment of conformation of the enzyme active center.

In the case of the interaction of Fpg with AP substrate, initial fragments of kinetic curves of Trp and 2-aPu fluorescence intensity characterizing the binding stages

have identical features towards F ligand and AP substrate (Fig. 7, b and c). This points to identical nature of the processes taking place at these stages. However, in the case of AP substrate, after formation of catalytically active complex, two β -elimination reactions leading to the formation of Fpg–product complex occur along with the following stage of complex dissociation. These additional stages result in appearance on kinetic curves of a phase of growth of Trp and 2-aPu fluorescence intensities. It is seen on kinetic curves that two chemical stages of the process are characterized by one stage of the fluorescence intensity increase.

The minimal kinetic Scheme 6, describing the kinetic curves, includes four equilibria corresponding to formation of catalytically active complex, the irreversible stage of chemical reactions, and subsequent dissociation of enzyme–product complex [E • P]:



The essence of processes taking place at stages of AP substrate binding is similar to those previously found for F ligand. Formation of catalytically active complex $[E \cdot AP]4$ later results in the chemical stages of the enzymatic process and the stage of dissociation of $[E \cdot P]$ enzyme–product complex.

Data obtained for G and F ligands and for AP substrate served as the basis for analysis of the most complex process of enzyme interaction with specific oxoG substrate. The main distinction of oxoG substrate is that the oxoG residue recognition and its interaction with the enzyme active center is added to the above-described binding stages.

Comparison of kinetic curves of Trp fluorescence intensity change for AP and oxoG substrates presented in Figs. 7c and 7d shows that in the case of oxoG substrate in the time interval 0.1–2.0 sec an additional stage is registered, which is absent from the interaction of Fpg with AP substrate.

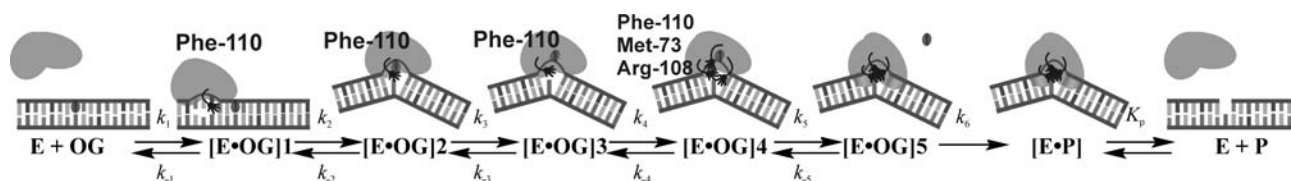
Mathematical analysis of data attributed to Trp fluorescence led to kinetic Scheme 7 containing five equilibrium stages that characterize binding of oxoG substrate [97]. Molecular transformations at these stages are evidently analogous to those previously described for AP substrate, while an additional stage characterizes the damaged base extruding from the DNA helix into the recess of the enzyme active center. The presence of *N*-glycosylase reaction resulted in five times reduction of the last chemical stage rate constant that in the case of AP substrate was $k_5 = 0.2 \text{ sec}^{-1}$ and in the case of oxoG substrate $k_6 = 0.04 \text{ sec}^{-1}$ (Table 4).

In the catalytically active complex bases localized at the 3' and 5' sides from oxoG interact with amino acid residues of the enzyme. Residues Met73 and Phe110 are incorporated at the 3' side, whereas Arg108 interacts with the 5' side (Fig. 6). Owing to this, in experiments with flu-

orescent analog of oxoG substrate two duplexes were used which carried an 2-aPu residue at the 3' or 5' side from oxoG (oxoG-aPu and aPu-oxoG, respectively). The resulting kinetic curves (Fig. 7d) revealed that the initial change of DNA structure takes place after nonspecific complex formation and characterizes duplex destabilization as in the case of nonspecific DNA. The second registered stage during 0.1–5.0 sec includes incorporation into the duplex of amino acid residues and formation of catalytically active complex. An important distinction of kinetic curves in this region is insignificant delay of the phase of lowering the fluorescence intensity for aPu-oxoG substrate. Such shift shows that amino acid residues of the enzyme are not simultaneously incorporated into DNA duplex as in the case of F ligand and AP substrate, namely, Arg108 interacting with the base localized at the 5' side from the damage is the last to be incorporated into the duplex, after Met73 and Phe110.

The rate of enzymatic reaction was also measured by a standard method in experiments with ^{32}P -labeled oxoG substrate by product separation in PAGE [97]. The rate constant k_{cat} obtained using this technique was $0.029 \pm 0.005 \text{ sec}^{-1}$, i.e. it was close to that of the irreversible stage k_6 . Besides, the constant of the dissociation of the enzyme–product $[E \cdot P]$ complex was determined by the fluorescent titration technique and appeared to be equal to $(5.3 \pm 0.4) \cdot 10^{-6} \text{ M}$, which is only twice higher than the K_p value obtained from analysis of the fluorescence kinetic curves. Thus, the values of constants agree well with those determined by the stopped-flow technique (Table 4).

We have shown in [99] using the “quench-flow” technique that kinetic curves of accumulation of the DNA strand break products are characterized by existence of a “burst” phase. In this case, during the pre-steady-state period of reaction under conditions of enzyme single turnover the identical Fpg activity was registered towards oxoG and AP substrates, i.e. cleaves of both DNA substrates occurred with identical rates, whereas during the steady-state period the rate of reaction with AP substrate was twice that with oxoG substrate. First, these data show that the limiting step of the enzy-



Kinetic scheme characterizing binding of oxoG substrate with *E. coli* Fpg [97], where E is Fpg enzyme from *E. coli*; OG is DNA substrate; $[E \cdot OG]1$ is primary enzyme complex with DNA substrate; $[E \cdot OG]2$ is enzyme complex with DNA substrate in which oxoG recognition and duplex distortion take place; $[E \cdot OG]3$ is enzyme complex with DNA substrate in which oxoG base is extruded from the duplex; $[E \cdot OG]4$ is incorporation of amino acid residues Phe110, Met73, and Arg108 into DNA duplex, formation of catalytically active complex, *N*-glycosylase reaction; $[E \cdot OG]5$ is enzyme complex with intermediate DNA product, release of free base oxoG, reactions of β - and δ -elimination; $[E \cdot P]$ is enzyme complex with DNA product

Scheme 7

Table 4. Rate constants characterizing enzyme conformational changes during the interaction of Fpg with DNA substrates

Constant	oxoG	AP	F	G
$k_1, \text{M}^{-1}\cdot\text{sec}^{-1}$	$(320 \pm 15) \cdot 10^6$	$(800 \pm 30) \cdot 10^6$	$(150 \pm 20) \cdot 10^6$	$(230 \pm 40) \cdot 10^6$
k_{-1}, sec^{-1}	890 ± 25	250 ± 20	270 ± 15	2700 ± 200
k_2, sec^{-1}	250 ± 18	36 ± 3	6.0 ± 0.2	
k_{-2}, sec^{-1}	2.4 ± 0.4	65 ± 8	0.02 ± 0.005	
k_3, sec^{-1}	6.7 ± 0.8	10.0 ± 0.5	10.0 ± 0.6	
k_{-3}, sec^{-1}	46 ± 0.6	40 ± 4	0.6 ± 0.1	
k_4, sec^{-1}	9.1 ± 0.6	11.0 ± 0.8	0.04 ± 0.007	
k_{-4}, sec^{-1}	2.4 ± 0.2	1.0 ± 0.1	0.01 ± 0.001	
k_5, sec^{-1}	0.20 ± 0.01	0.20 ± 0.01		
k_{-5}, sec^{-1}				
k_6, sec^{-1}	0.04 ± 0.006			
K_p, M	$(2.0 \pm 0.3) \cdot 10^{-6}$	$(1.8 \pm 0.3) \cdot 10^{-6}$		

matic process is the enzyme release from its complex with the product. It was shown using the MS/ESI technique [99] that the really limiting step of the process is decomposition of the Fpg covalent adduct with ribose residue resulting from β, δ -elimination reactions (Fig. 5). Second, the rate of enzyme release from the enzyme–product complex must depend on the presence/absence in the enzyme active center of 8-oxoguanine residue removed during the glycosylase reaction. A similar conclusion concerning the removed base effect on the rate of enzyme turnover has been recently reported by Adhikari et al. [100], who studied the mechanism of action of human N-methylpurine-DNA glycosylase. In the case of Fpg the presence in the enzyme active center of removed 8-oxoguanine should decrease the rate of decomposition of Fpg covalent adduct with ribose residue and thus to decrease the rate of enzyme turnover [99].

Thus, it can be concluded that formation of catalytically active Fpg complex with specific DNA substrate includes at least five steps during which coordinated conformational transformations in protein and DNA molecules occur. Primary nonspecific binding results in formation of a collision complex with DNA. Formation of a second complex plays the key role in recognition of damaged region in DNA. When specific substrate is localized in the enzyme-binding site, the third stage of the process occurs, the extrusion of the damaged base. This step results in formation of a recess in the DNA duplex. The fourth step characterizes incorporation of the enzyme amino acid residues into the formed recess. After that conformation of the enzyme active center is adjusted and catalytic steps of the process occur. The enzymatic cycle is completed by dissociation of the enzyme–product complex after which the enzyme initially remains bound

to a ribose residue, although its conformation corresponds to the free enzyme. Dissociation of the Fpg covalent adduct with the ribose residue is the limiting stage of the whole enzymatic process; it is not seen under conditions of “stopped-flow” experiments with fluorimetric detection, but it follows from “quench-flow” data and is registered using MS/ESI analysis [99].

Data in the literature of the last 10–15 years are indicative of increased interest in study of fine aspects of mechanisms of enzymatic reactions. Significant progress in this direction is due largely to development of X-ray analysis, site-directed mutagenesis, methods of fast kinetics, etc. New technical resources of present-day physico-chemical and chemical methods make it possible to register separate elementary steps of enzyme action. Combination of data obtained by various methods reveals the detailed kinetic mechanisms of enzymatic processes and identifies the molecular nature of all stages.

Examples of molecular-kinetic mechanisms of action of enzymes interacting with DNA make it possible to distinguish some general features of enzymatic processes. As a rule, formation of the primary enzyme–substrate complexes is a very fast process. However, stability of these complexes is not very high and they either dissociate or undergo a series of conformational changes resulting in their stabilization. Such conformational changes take place both in the enzyme and in the DNA substrate molecules. These changes result in formation of highly specific interactions between enzymes and substrates, which, as a rule, result in discrimination between substrates and “non-substrates”. Further conformational changes in enzyme–substrate complexes result in emergence of the catalytically active state in which structures of interacting molecules are optimized for chemical

stages of the processes. Mechanisms of these processes correspond to Koshland's model of "induced fit" [101]. Thus, combination of pre-steady-state kinetics with registration of conformational dynamics makes it possible to identify elementary stages of substrate recognition by enzymes and transformation to products.

This work was supported by President Grant MK-1304.2010.4, Russian Foundation for Basic Research grants No. 10-04-00070 and No. 08-04-12211, state contracts 02.740.11.0079 and 02.740.11.5012, and integration projects of Siberian Branch of the Russian Academy of Sciences No. 28 and 48.

REFERENCES

- Hammes, G. G. (2002) *Biochemistry*, **41**, 8221-8228.
- Boehr, D. D., Dyson, H. J., and Wright, P. E. (2006) *Chem. Rev.*, **106**, 3055-3079.
- Olsson, M. H. M., Parson, W. W., and Warshel, A. (2006) *Chem. Rev.*, **106**, 1737-1756.
- Giraldo, J., Roche, D., Rovira, X., and Serra, J. (2006) *FEBS Lett.*, **580**, 2170-2177.
- Agarwa, P. K. (2005) *J. Am. Chem. Soc.*, **127**, 15248-15256.
- Eisenmesser, E. Z., Millet, O., Labeikovsky, W., Korzhnev, D. M., Wolf-Watz, M., Bosco, D. A., Skalicky, J. J., Kay, L. E., and Kern, D. (2005) *Nature*, **438**, 117-121.
- Eisenmesser, E. Z., Bosco, D. A., Akke, M., and Kern, D. (2002) *Science*, **295**, 1520-1523.
- Garcia-Viloca, M., Gao, J., Karplus, M., and Truhlar, D. G. (2004) *Science*, **303**, 186-195.
- Cantor, Ch., and Shimmel, P. (1980) *Biophysical Chemistry: Part I: The Conformation of Biological Macromolecules*, W.H. Freeman & Company, San Francisco.
- Keleti, T. (1988) *Basic Enzyme Kinetics*, Akademiai Kiado, Budapest.
- Cornish-Bowden, A. (2004) *Fundamentals of Enzyme Kinetics, 3rd Edn.*, Portland Press Ltd, London.
- Cantor, Ch., and Shimmel, P. (1980) *Biophysical Chemistry: Part III: The Behavior of Biological Macromolecules*, W.H. Freeman & Company, San Francisco.
- Berezin, I. V., and Martinek, K. (1977) *Bases of Physical Chemistry of Enzyme Catalysis* [in Russian], Izd-vo Vysshaya Shkola, Moscow.
- Johnson, K. A. (1992) *Enzymes*, **20**, 1-61.
- Varfolomeev, S. D., and Gurevich, K. G. (1999) *Biokinetics: Practical Course* [in Russian], FAIR-PRESS, Moscow.
- Caldin, E. F. (1964) *Fast Reactions in Solution*, Blackwell Scientific, Oxford.
- Hammes, G. G. (1974) *Investigation of Elementary Reaction Steps in Solution and Very Fast Reactions*, Wiley, New York.
- Lakowicz, J. (1983) *Principles of Fluorescence Spectroscopy*, Plenum Press, New York.
- Dunlap, C. A., and Tsai, M. D. (2002) *Biochemistry*, **41**, 11226-11235.
- Cherepanov, A. V., and de Vries, S. (2001) *Biophys. J.*, **81**, 3545-3559.
- Wong, I., Lundquist, A. J., Bernards, A. S., and Mosbaugh, D. W. (2002) *J. Biol. Chem.*, **277**, 19424-19432.
- Watanabe, S. M., and Goodman, M. F. (1982) *Proc. Natl. Acad. Sci. USA*, **79**, 6429-6433.
- Sowers, L. C., Fazakerley, G. V., Eritja, R., Karlan, B. E., and Goodman, M. F. (1986) *Proc. Natl. Acad. Sci. USA*, **83**, 5434-5438.
- Rachofsky, E. L., Osman, R., and Ross, J. B. A. (2001) *Biochemistry*, **40**, 946-956.
- Purohit, V., Grindley, N. D. F., and Joyce, C. M. (2003) *Biochemistry*, **42**, 10200-10211.
- Fiala, K. A., Abdel-Gawad, W., and Suo, Z. (2004) *Biochemistry*, **43**, 6751-6762.
- Jia, Y., Kumar, A., and Patel, S. S. (1996) *J. Biol. Chem.*, **271**, 30451-30458.
- Mandal, S. S., Fidalgo da Silva, E., and Reha-Krantz, L. J. (2002) *Biochemistry*, **41**, 4399-4406.
- Yang, G., Wang, J., and Konigsberg, W. (2005) *Biochemistry*, **44**, 3338-3346.
- Evdokimov, A. A., Zinoviev, V. V., Malygin, E. G., Schlagman, S. L., and Hattman, S. (2002) *J. Biol. Chem.*, **277**, 279-286.
- Wallace, S. S. (2002) *Free Radic. Biol. Med.*, **33**, 1-14.
- Marnett, L. J. (2000) *Carcinogenesis*, **21**, 361-370.
- Dizdaroglu, M., Jaruga, P., Birincioglu, M., and Rodriguez, H. (2002) *Free Radic. Biol. Med.*, **32**, 1102-1115.
- Boiteux, S., and Guillet, M. (2004) *DNA Repair (Amst)*, **3**, 1-12.
- Cooke, M. S., Evans, M. D., Dizdaroglu, M., and Lunec, J. (2003) *FASEB J.*, **17**, 1195-1214.
- Evans, M. D., Dizdaroglu, M., and Cooke, M. S. (2004) *Mutat. Res.*, **567**, 1-61.
- Xie, Y., Yang, H., Cunanan, C., Okamoto, K., Shibata, D., Pan, J., Barnes, D. E., Lindahl, T., McIlhatton, M., Fishel, R., and Miller, J. H. (2004) *Cancer Res.*, **64**, 3096-3102.
- Wan, J., Bae, M.-A., and Song, B.-J. (2004) *Exp. Mol. Med.*, **36**, 71-77.
- Gu, Y., Desai, T., Gutierrez, P. L., and Lu, A.-L. (2001) *Med. Sci. Monit.*, **7**, 861-868.
- Raha, S., and Robinson, B. H. (2000) *Trends Biochem. Sci.*, **25**, 502-508.
- Beckman, K. B., and Ames, B. N. (1998) *Physiol. Rev.*, **78**, 547-581.
- Parikh, S. S., Mol, C. D., and Tainer, J. A. (1997) *Structure*, **5**, 1543-1550.
- Iyer, R. R., Pluciennik, A., Burdett, V., and Modrich, P. L. (2006) *Chem. Rev.*, **106**, 302-323.
- Shin, D. S., Chahwan, C., Huffman, J. L., and Tainer, J. A. (2004) *DNA Repair (Amst)*, **3**, 863-873.
- Krokan, H. E., Nilsen, H., Skorpen, F., Otterlei, M., and Slupphaug, G. (2000) *FEBS Lett.*, **476**, 73-77.
- Memisoglu, A., and Samson, L. (2000) *Mutat. Res.*, **451**, 39-51.
- Wilson III, D. M., and Barsky, D. (2001) *Mutat. Res.*, **485**, 283-307.
- Kubota, Y., Nash, R. A., Klungland, A., Schar, P., Barnes, D. E., and Lindahl, T. (1996) *EMBO J.*, **15**, 6662-6670.
- Pascucci, B., Maga, G., Hubscher, U., Bjoras, M., Seeberg, E., Hickson, I. D., Villani, G., Giordano, C., Cellai, L., and Dogliotti, E. (2002) *Nucleic Acids Res.*, **30**, 2124-2130.
- Dodson, M. L., Michaels, M. L., and Lloyd, R. S. (1994) *J. Biol. Chem.*, **269**, 32709-32712.

51. Dodson, M. L., and Lloyd, R. S. (2002) *Free Radic. Biol. Med.*, **32**, 678-682.
52. Demple, B., and Sung, J.-S. (2005) *DNA Repair (Amst.)*, **4**, 1442-1449.
53. Stivers, J. T., and Jiang, Y. L. (2003) *Chem. Rev.*, **103**, 2729-2759.
54. Krokan, H. E., Standal, R., and Slupphau, G. (1997) *Biochem. J.*, **325**, 1-16.
55. Zharkov, D. O., and Grollman, A. P. (2005) *Mutat. Res.*, **577**, 24-54.
56. Fromme, J. C., Banerjee, A., and Verdine, G. L. (2004) *Curr. Opin. Struct. Biol.*, **14**, 43-49.
57. Zharkov, D. O., Shoham, G., and Grollman, A. P. (2003) *DNA Repair (Amst.)*, **2**, 839-862.
58. Pearl, L. H. (2000) *Mutat. Res.*, **460**, 165-181.
59. Denver, D. R., Swenson, S. L., and Lynch, M. (2003) *Mol. Biol. Evol.*, **20**, 1603-1611.
60. David, S. S., and Williams, S. D. (1998) *Chem. Rev.*, **98**, 1221-1261.
61. Krokan, H. E., Drablos, F., and Slupphaug, G. (2002) *Oncogene*, **21**, 8935-8948.
62. Mol, C. D., Arvai, A. S., Slupphaug, G., Kavli, B., Alseth, I., Krokan, H. E., and Tainer, J. A. (1995) *Cell*, **80**, 869-878.
63. Parikh, S. S., Mol, C. D., Slupphaug, G., Bharati, S., Krokan, H. E., and Tainer, J. A. (1998) *EMBO J.*, **17**, 5214-5226.
64. Parikh, S. S., Walcher, G., Jones, G. D., Slupphaug, G., Krokan, H. E., Blackburn, G. M., and Tainer, J. A. (2000) *Proc. Natl. Acad. Sci. USA*, **97**, 5083-5088.
65. Saikrishnan, K., Sagar, M. B., Ravishankar, R., Roy, S., Purnapatre, K., Handa, P., Varshney, U., and Vijayan, M. (2002) *Acta Crystallogr. D Biol. Crystallogr.*, **58**, 1269-1276.
66. Stivers, J. T., Pankiewicz, K. W., and Watanabe, K. A. (1999) *Biochemistry*, **38**, 952-963.
67. Jiang, Y. L., Stivers, J. T., and Song, F. (2002) *Biochemistry*, **41**, 11248-11254.
68. Jiang, Y. L., and Stivers, J. T. (2002) *Biochemistry*, **41**, 11236-11247.
69. Cadet, J., Berger, M., Douki, T., and Ravanat, J. L. (1991) *Rev. Physiol. Biochem. Pharmacol.*, **131**, 1-87.
70. Dizdaroglu, M. (1991) *Free Radic. Biol. Med.*, **10**, 225-242.
71. Bernards, A. S., Miller, J. K., Bao, K. K., and Wong, I. (2002) *J. Biol. Chem.*, **277**, 20960-20964.
72. Kasai, H., and Nishimura, S. (1984) *Nucleic Acids Res.*, **12**, 2137-2145.
73. Shibutani, S., Takeshita, M., and Grollman, A. P. (1991) *Nature*, **349**, 431-434.
74. Grollman, A. P., and Moriya, M. (1993) *Trends Genet.*, **9**, 246-249.
75. Michaels, M. L., and Miller, J. H. (1992) *J. Bacteriol.*, **174**, 6321-6325.
76. Fowler, R. G., White, S. J., Koyama, C., Moore, S. C., Dunn, R. L., and Schaaper, R. M. (2003) *DNA Repair (Amst.)*, **2**, 159-173.
77. Sakumi, K., Furuichi, M., Tsuzuki, T., Kakuma, T., Kawabata, S., Maki, H., and Sekiguchi, M. (1993) *J. Biol. Chem.*, **268**, 23524-23530.
78. Slupska, M. M., Baikalov, C., Luther, W. M., Chiang, J.-H., Wei, Y.-F., and Miller, J. H. (1996) *J. Bacteriol.*, **178**, 3885-3892.
79. Lu, A.-L., Tsai-Wu, J.-J., and Cillo, J. (1995) *J. Biol. Chem.*, **270**, 23582-23588.
80. Bulychev, N. V., Varaprasad, C. V., Dorman, G., Miller, J. H., Eisenberg, M., Grollman, A. P., and Johnson, F. (1996) *Biochemistry*, **35**, 13147-13156.
81. Guan, Y., Manuel, R. C., Arvai, A. S., Parikh, S. S., Mol, C. D., Miller, J. H., Lloyd, R. S., and Tainer, J. A. (1998) *Nat. Struct. Biol.*, **5**, 1058-1064.
82. Fromme, J. C., Banerjee, A., Huang, S. J., and Verdine, G. L. (2004) *Nature*, **427**, 652-656.
83. Zharkov, D. O., Gilboa, R., Yagil, I., Kycia, J. H., Gerchman, S. E., Shoham, G., and Grollman, A. P. (2000) *Biochemistry*, **39**, 14768-14778.
84. Lu, A.-L., Yuen, D. S., and Cillo, J. (1996) *J. Biol. Chem.*, **271**, 24138-24143.
85. Williams, S. D., and David, S. S. (1998) *Nucleic Acids Res.*, **26**, 5123-5133.
86. Williams, S. D., and David, S. S. (1999) *Biochemistry*, **38**, 15417-15424.
87. Wright, P. M., Yu, J., Cillo, J., and Lu, A.-L. (1999) *J. Biol. Chem.*, **274**, 29011-29018.
88. Manuel, R. C., Hitomi, K., Arvai, A. S., House, P. G., Kurtz, A. J., Dodson, M. L., McCullough, A. K., Tainer, J. A., and Lloyd, R. S. (2004) *J. Biol. Chem.*, **279**, 46930-46939.
89. Porello, S. L., Leyes, A. E., and David, S. S. (1998) *Biochemistry*, **37**, 14756-14764.
90. Chmiel, N. H., Golinelli, M. P., Francis, A. W., and David, S. S. (2001) *Nucleic Acids Res.*, **29**, 553-564.
91. McCann, J. A. B., and Berti, P. J. (2003) *J. Biol. Chem.*, **278**, 29587-29592.
92. Tchou, J., and Grollman, A. P. (1995) *J. Biol. Chem.*, **270**, 11671-11677.
93. Zharkov, D. O., Rieger, R. A., Iden, C. R., and Grollman, A. P. (1997) *J. Biol. Chem.*, **272**, 5335-5341.
94. Bhagwat, M., and Gerlt, J. A. (1996) *Biochemistry*, **35**, 659-665.
95. Gilboa, R., Zharkov, D. O., Golan, G., Fernandes, A. S., Gerchman, S. E., Matz, E., Kycia, J. H., Grollman, A. P., and Shoham, G. (2002) *J. Biol. Chem.*, **277**, 19811-19816.
96. Fedorova, O. S., Nevinsky, G. A., Koval, V. V., Ishchenko, A. A., Vasilenko, N. L., and Douglas, K. T. (2002) *Biochemistry*, **41**, 1520-1528.
97. Koval, V. V., Kuznetsov, N. A., Zharkov, D. O., Ishchenko, A. A., Douglas, K. T., Nevinsky, G. A., and Fedorova, O. S. (2004) *Nucleic Acids Res.*, **32**, 926-935.
98. Kuznetsov, N. A., Koval, V. V., Zharkov, D. O., Vorobiev, Y. N., Nevinsky, G. A., Douglas, K. T., and Fedorova, O. S. (2007) *Biochemistry*, **46**, 424-435.
99. Kuznetsov, N. A., Zharkov, D. O., Koval, V. V., Buckle, M., and Fedorova, O. S. (2009) *Biochemistry*, **48**, 11335-11343.
100. Adhikari, S., Uren, A., and Roy, S. (2009) *DNA Repair (Amst)*, **8**, 1201-1206.
101. Koshland, D. E. (1960) *Adv. Enzymol.*, **22**, 45-97.